Geotech Geol Eng
DOI 10.1007/s10706-017-0186-z

ORIGINAL PAPER

Bearing Capacity of the New Composite Foundation with Discrete Material-Concrete Compound Piles

Youlin Guo · Minghua Zhao · Guihai Fu · Yongsuo Li · Pengfei Yu

Received: 20 October 2016 / Accepted: 7 February 2017

Abstract In order to solve the bulging deformation and fracture at the top of widely used gravel piles in treating ground consolidation, a new, optimized composite foundation form was proposed. The composite foundation was constructed using discrete materials and concrete piles. Additionally, various parameters of this new composite foundation were analyzed, including foundation forms, construction technologies, bearing mechanism and failure mode. By applying cavity expansion theory, the Vesic cavity spreading pressure of the discrete material-concrete pile is solved as a polar axis symmetric problem on the basis of Mohr–Coulomb yield criterion. Then the computing formula for the ultimate bearing capacity of the discrete materials-concrete pile is elicited when the internal friction angle of soil in the piles is $\varphi = 0$ and $\varphi \neq 0$. Finally, the ultimate bearing capacity value of the composite foundation is acquired through analytic calculation and numerical simulation. Finally, it is found that the calculation result is 14.4% lower than that of the simulated result, which is within the acceptable accuracy range and therefore proves the accuracy of the analytic calculation method for bearing capacity of the new composite foundation.

Keywords Composite foundation · Discrete material · Concrete · Bearing capacity · Numerical calculation

1 Introduction

It has been over 200 years since European engineers first applied gravel piles to consolidate sedimentary soft soil in the early nineteenth century (Hughes and Withers 1974). The technology has been widely used and rapidly developed in the consolidation treatment of soft soil foundation. The lateral constraining force generated by gravel piles constrained by the confining forces of surrounding soil can to a certain extent improve the bearing capacity of the composite foundation of gravel piles. However, bulging damage, overall shear or sliding failure, and punching failure frequently occur on gravel pile composite foundations (Zhao et al. 2011). In addition, the lateral constraint is low due to the swallow burial depth so that bulging deformation failure happens within the pile top in the depth one to three times of the pile diameter (Murugesan and Rajagopal 2009).

Y. Guo (✉) · M. Zhao
Geotechnical Engineering Institute, Hunan University, Changsha 410082, China
e-mail: guoyoulin82@163.com

Y. Guo · G. Fu · Y. Li
College of Civil Engineering, Hunan City University, Yiyang 413000, China

P. Yu
Yiyang City Highway Administration Bureau of Hunan Province, Yiyang 413000, China

Published online: 13 February 2017

To solve this problem, numerous scholars have carried out lots of researches on consolidation technologies of new gravel pile composite foundations. For example, composite foundations of discrete gravel materials with horizontal multilayer reinforcement, that is, foundations with multilayer geotechnical grilles well restrict the lateral deformation (Alamgir et al. 1996; Poorooshasb et al. 1996; Hasan et al. 2012). Piles are wrapped by using sleeves made from synthetic materials and hoop stirrups are set to restrict bulging deformation (Zhou and Zhang 1997; Zhuang et al. 2016). In addition, composite foundations of discrete gravel materials with geotechnical grilles set on the top of foundations for reinforcement show better bearing capacities than those of ordinary gravel pile composite foundations (Wang and Pi 2011; Deb and Mohapatra 2013).

Aiming at the characteristic that bulging deformation is likely to occur on the top of gravel piles, the study puts forward a consolidation technology for the new composite foundation to further enrich the theory and engineering practice of gravel pile composite foundations. The new composite foundation is constructed by pouring concrete into the upper part of the gravel pile to make the concrete grout permeate to the bottom of the gravel piles, thus forming a concrete-gravel pile composite foundation. The proposal of the new composite foundation supplements the theoretical research system of composite foundations and provides important theoretical reference and engineering guiding significance.

2 New Composite Foundation with Discrete Material-Concrete Compound Piles

2.1 Composite Foundation Form

The newly proposed composite foundation is formed according to the following process: Gravel compaction piles are on the bottom of discrete material piles, while concrete is poured from the upper part to form concrete piles. The concrete grout poured into the bottom of the piles permeates into the gravel piles to form effective connection so as to form the composite foundation with discrete material-concrete piles. The new composite foundation with discrete material-concrete piles is shown in Fig. 1.

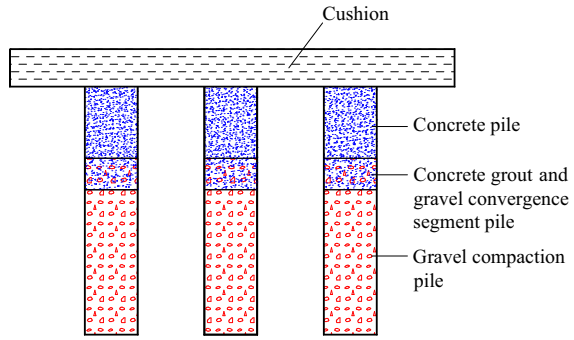

Fig. 1 New composite foundation with discrete material-concrete piles

2.2 Construction Technology

In the precondition of improving pile strength as well as vertical and horizontal bearing capacities, the new discrete material-concrete compound pile also decreases project cost. In addition, the compound pile also has other advantages, such as simple construction technology and strong practicability. The constructing process is shown as Fig. 2 and the specific construction technology is as follow:

1. Pile position is determined through measuring and setting out and then the sinking tube with valve stopper is put at specified position, as shown in Fig. 2a.
2. After turning on the bobbing machine, the sinking tube is pounded to the designed depth in the soil. Every time after the tube sinks by 0.5 m, the pounding is stopped to vibrate the sinking tube for 1 min, as illustrated in Fig. 2b.
3. A certain amount of gravels are poured into the tube cavity, as shown in Fig. 2c.

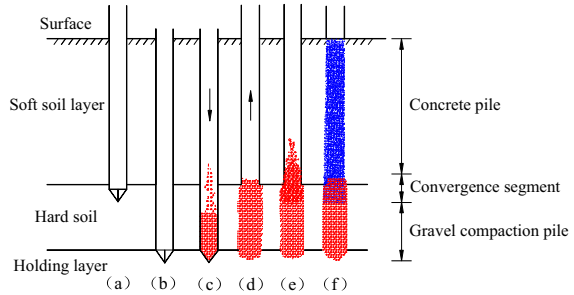

Fig. 2 Construction technology of new composite foundation with discrete material-concrete piles

4. Then the bobbing machine is turned on to pull the sinking tube out at the rate within 0.5–1.5 m/min, during which the tube is vibrated for 1 min every being pulled out by 1 m, as shown in Fig. 2d.
5. The procedures in Fig. 2c, d are repeated until the sinking tube is pulled out to the specified height of the gravel section. Then the gravels are poured into the tube and compacted through vibration, as demonstrated in Fig. 2e.
6. The bobbing machine is turned on again to pull the entire sinking tube out. At this moment, concrete is poured into the tube till reaching the ground level to form a concrete section, as shown in Fig. 2f.

In this way, a gravel discrete material-concrete tandem compound pile is formed.

2.3 Bearing Mechanism

The bearing mechanism of the composite foundation with discrete material-concrete piles is not simple superposition of discrete materials and concrete. However, it is an organic whole of discrete materials, concrete, and surrounding soil constructed by the permeation of concrete grout to a certain depth of the discrete materials to effectively connect with the latter. Therefore, the compositions are deformed compatibly and bear stress jointly.

When vertical loads are applied on the composite foundation with discrete material-concrete piles, the pile and the surrounding soil are under three-dimensional stresses. Owing to the upper part of the pile containing concrete shows favorable cementing property and stiffness, it does not need the surrounding soil to offer obvious confining strength and therefore effectively prevents the top of the pile from bulging failure. As to the lower gravel pile, it is subjected to the vertical load effect passed by the upper concrete pile. Due to the lack of cementing property, the discrete gravel materials are rapidly laterally deformed. However, the resistance of the surrounding soil to the bulging of the pile increases with the growing depth, effectively restricting the circumferential deformation of the pile and thereby improving the bearing capacity of the composite foundation. When the upper pile exerts a large load effect and the surrounding soil is weak, a reinforcement cage can be set up while pouring concrete in the upper pile to improve the horizontal tensile strength of the upper concrete pile. Thus, the composite foundation with discrete material-reinforced concrete piles is formed.

2.4 Failure Mode

The failure forms of traditional composite foundations with piles built using discrete gravel materials include bulging failure, overall shear or sliding failure, and punching failure. Compared with traditional piles built using discrete gravel materials, the discrete material-concrete pile proposed by the study general does not experience overall sliding failure and upper bulging failure due to the larger stiffness and shear strength of the upper concrete. In addition, the punching failure is not likely to happen once the pile body is built in hard bearing layers. Therefore, it is speculated that the position of gravel bulging probably downward shifts due to the existence of the concrete section. As a result, lateral bulging or shear sliding failure probably occur on the connecting section and deep gravel pile below the concrete pile, as shown in Fig. 3. In view of this, the study analyzes the ultimate bearing capacity of the new composite foundation with discrete material-concrete pile under the failure mode at the site.

2.5 Calculation Steps of Bearing Capacities

Bearing capacity Q_{cf} of the new composite foundation with compound pile constructed using discrete materials and concrete can be calculated through the following three steps: first, the bearing capacity Q_p of the compound piles is calculated. Second is to compute the bearing capacity Q_s of surrounding soil

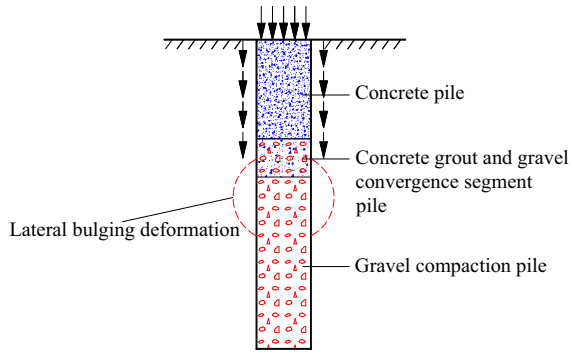

Fig. 3 Failure modes of the new discrete material-concrete piles

of the discrete material-concrete compound pile. Third, bearing capacity Q_{cf} of the composite foundation with the discrete material-concrete compound pile is calculated.

3 Calculation of Bearing Capacities of the Piles

Based on Mohr–Coulomb yield criterion, the bearing capacity of the new, compound pile constructed using discrete materials and concrete is analyzed and calculated by using cavity expansion theory.

3.1 Building the Calculation Model

Due to the enhanced tensile strength and cementing bond of the upper concrete section compared with those of traditional gravel piles, the lateral deformation of the discrete material-concrete piles can be constrained so as to improve the ultimate bearing capacities. The surrounding soil and the piles of composite foundation support loads together when the composite foundation is affected by upper load effect. In addition, the bearing capacity of piles depends on the confining constraint for lateral bugling and shear sliding failure occurring on the connecting section and gravel pile below the concrete section after the gravel bulging position downward shifts. Based on the characteristic, the calculation model is shown in Fig. 4.

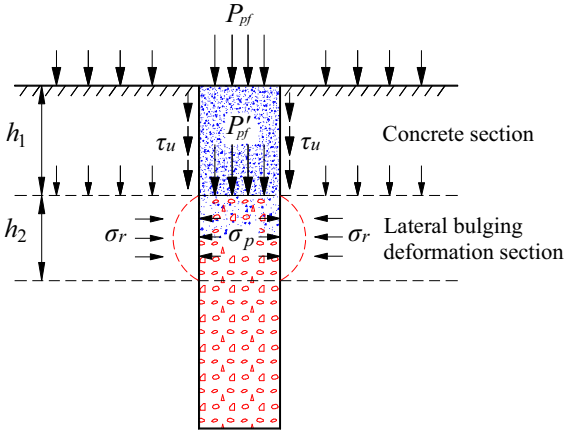

Fig. 4 Calculation model for the bearing capacity of the discrete material-concrete pile

3.2 Basic Assumption

To simply the calculation for the bearing capacity of the new discrete material-concrete compound pile, it is assumed as follows (Grujicic et al. 2013):

1. Surrounding soil of piles is a homogeneous and isotropic ideal elastoplastic body.
2. Piles conform to the Mohr–Coulomb strength theory when they are at the limit equilibrium state under the effect of vertical loads. In addition, the calculation model is axisymmetric.
3. Bulging failure is not likely to happen on concrete section due to strong bonding strength, while radial bulging and shear sliding failure occur on gravel section.

3.3 Side Friction of Concrete Section

According to the mechanical model in Fig. 4, stresses on the discrete material-concrete pile can be divided into the concrete section and the lateral bulging deformation section. When the top of the pile is affected by the ultimate external load Q_p of the ground, the concrete section is influenced by the ultimate external load Q_p and the side friction τ_u (shear force) between the soil and the pile. The load Q'_p is passed to the lateral bugling deformation section of the lower gravel pile through the concrete section. Therefore, the concrete section plays a dual role in sharing loads and resisting deformation in the vertical and radical directions. The mechanical expression is shown as Formula (1).

$$Q_p = Q'_p + \tau_u \tag{1}$$

Ultimate friction stress τ_u in the concrete section is distributed as a straight line along the pile (Brauns 1978).

$$\tau_u = \alpha C_u \tag{2}$$

where α is the reduction coefficient ($\alpha = 0.3$–1.0) and C_u represents undrained shear strength of the soil mass.

The lateral bugling deformation section starts to be radically deformed until bulges under the load Q'_p passed from the concrete section. Therefore, the ultimate bearing capacity of the discrete material-

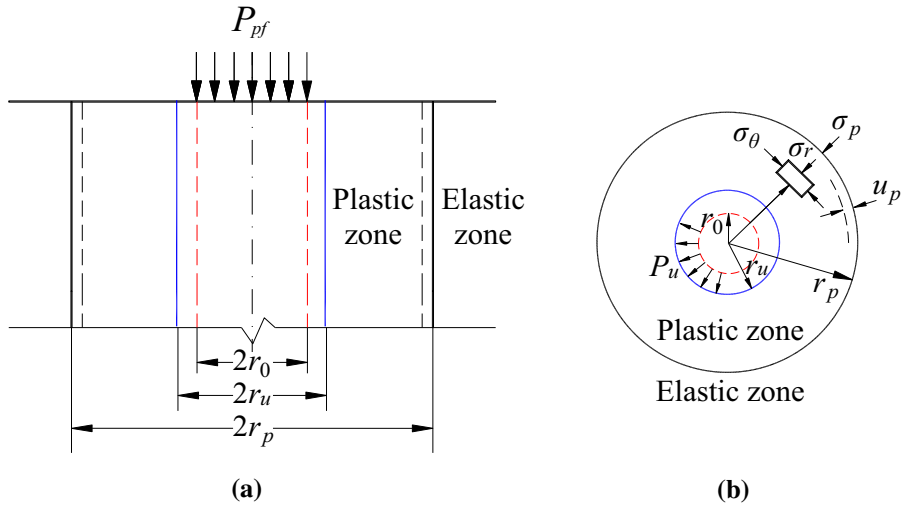

Fig. 5 Mechanical analysis model based on cavity expansion theory

concrete pile is determined by the ultimate side resistance σ_r of the surrounding soil.

3.4 Ultimate Bearing Capacity of the Lateral Bugling Deformation Section

The ultimate side resistance σ_r of soil surrounding the lateral bulging deformation section is the ultimate cavity expansion stress of surrounding soil on the pile. In addition, by considering the force of the surrounding soil as the cavity expansion effect, the mechanical analysis model in Fig. 5 is built based on cavity expansion theory.

The surrounding soil gradually turns form elastic state into plastic state under the pressure of cavity expansion. When the soil reaches to an ultimate state, the radius of the circular cavity expands from the original r_0 to r_u. The radius of the plastic zone of the soil reaches to r_p and the ultimate pressure of cavity expansion is P_u. Considering that cavity expansion is a plain strain problem with symmetrical force axes, the Vesic cavity expansion pressure is solved by using polar coordinates. In addition, the stress state of the axially symmetric soil unit is built, as shown in Fig. 6.

According to force balance analysis, the differential equation for equilibrium plane strain on the point of the soil is obtained, as shown in Formula (3).

$$\frac{d\sigma_r}{dr}+\frac{\sigma_r-\sigma_\theta}{r}=0 \tag{3}$$

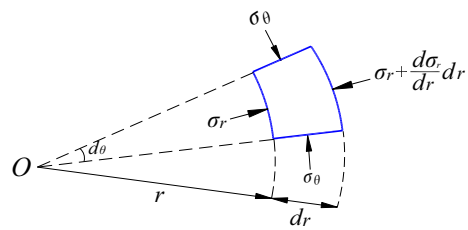

Fig. 6 Stress state of the axially symmetric soil unit

When the surrounding soil is in elastic state, the generalized Hooke law is presented as Formula (4).

$$\begin{aligned}\varepsilon_r&=\frac{1-v^2}{E}\left(\sigma_r-\frac{v}{1-v}\sigma_\theta\right)\\ \varepsilon_\theta&=\frac{1-v^2}{E}\left(\sigma_\theta-\frac{v}{1-v}\sigma_r\right)\end{aligned} \tag{4}$$

where E and V represent the elasticity modulus and the Poisson ratio of the surrounding soil, respectively. By employing the Mohr–Coulomb as the yield criterion, we can obtain

$$(\sigma_r-\sigma_\theta)=(\sigma_r+\sigma_\theta)\sin\varphi+2C\cos\varphi \tag{5}$$

Then, the conditions under which the internal friction of the surrounding soil is $\varphi=0$ and $\varphi\neq 0$ are analyzed. If $\varphi=0$, Formula (5) is converted to

$$(\sigma_r-\sigma_\theta)=2C \tag{6}$$

In the condition of axial symmetry, the radical displacement of unit soil in the elastic state is

$$u = \frac{(1+v)}{E} r\sigma_r \tag{7}$$

By substituting Formulae (6) into (3) to perform integral operation and introducing the boundary condition $r = r_u$, then $\sigma_r = P_u$ and the following is obtained:

$$\sigma_r = P_u - 2C \ln \frac{r}{r_u} \tag{8}$$

Formula (9) is obtained by substituting Formulae (8) into (6).

$$\sigma_\theta = P_u - 2C \ln \left(\frac{r}{r_u} + 1 \right) \tag{9}$$

When the internal friction of the soil is zero, the plastic volumetric strain during the cavity expansion of the soil is zero. Under such condition, the volume change of the circular cavity all occur to the elastic area. According to Fig. 5, the following formula can be obtained.

$$\pi r_u^2 - \pi r_0^2 = \pi r_p^2 - \pi (r_p - u_p)^2 \tag{10}$$

where u_p is the radical displacement at the boundary of elastic and plastic zones.

By solving Formula (10), we acquire

$$2u_p \frac{r_p}{r_u^2} = 1 \tag{11}$$

By introducing the boundary condition $r = r_p$, Formula (12) can be obtained.

$$u_p = \frac{(1+v)}{E} r_p \sigma_p \tag{12}$$

Combining with the yield criterion in Formula (6), following formula can be obtained when $r = r_p$:

$$\sigma_\theta = -\sigma_r = \sigma_p \tag{13}$$

According to Formulae (6) and (13), there is

$$\sigma_p = C \tag{14}$$

Based on Formulae (11) and (12), we obtain

$$\frac{2r_p^2}{r_u^2} \frac{(1+v)}{E} \sigma_p = 1 \tag{15}$$

By combining Formulae (14) and (15), we can get

$$\frac{r_p^2}{r_u^2} = \frac{E}{2(1+v)C} \tag{16}$$

Stiffness index I_r is introduced to simplify the expression.

$$I_r = \frac{E}{2(1+v)C} = \frac{G}{C_u} \tag{17}$$

where G and C_u represent the shear modulus and the undrained shear strength of the soil, and it is considered that $C = C_u$.

$$\frac{r_p}{r_u} = \sqrt{I_r} \tag{18}$$

By combining Formula (8) with the boundary condition $r = r_p$ at the boundary of elastic and plastic zones, the following formula is acquired:

$$\sigma_r = P_u - 2C \ln \frac{r_p}{r_u} \tag{19}$$

Finally, Formulae (14), (18) and (19) are combined to obtain the ultimate cavity expansion pressure P_u when the internal friction angle of the surrounding soil is $\varphi = 0$.

$$P_u = C(\ln I_r + 1) = C_u(\ln I_r + 1) \tag{20}$$

In the case that $\varphi \neq 0$, the volumetric strain of the plastic zone is not zero. Similarly, the ultimate cavity expansion pressure P_u can be deduced as:

$$P_u = (q + C\mathrm{ctg}\varphi)(1 + \sin\varphi)(I_r \sec\varphi)^{\frac{\sin\varphi}{1+\sin\varphi}} - C\mathrm{ctg}\varphi \tag{21}$$

where q represents the initial stress of the surrounding soil.

According to cavity expansion theory, the ultimate bearing capacity of the section with lateral bugling deformation potential of the gravel pile is

$$Q_p' = P_u \mathrm{tg}^2 \left(45^\circ + \frac{\varphi_p}{2} \right) \tag{22}$$

where φ_p represents the internal friction angle of the pile.

Therefore, the ultimate cavity expansion pressure P_u calculated in the above section is substituted into Formula (22) to compute the ultimate bearing capacities of the section with lateral bugling deformation potential when $\varphi = 0$ and $\varphi \neq 0$, as shown in the following formulae:

$$Q_p' = C_u(\ln I_r + 1)\mathrm{tg}^2 \left(45^\circ + \frac{\varphi_p}{2} \right) \tag{23}$$

$$Q_p' = \{(q + C\mathrm{ctg}\varphi)(1 + \sin\varphi)(I_r \sec\varphi)^{\frac{\sin\varphi}{1+\sin\varphi}} - C\mathrm{ctg}\varphi\} \times \mathrm{tg}^2\left(45^\circ + \frac{\varphi_p}{2}\right) \quad (24)$$

3.5 Calculation of Bearing Capacity Qp of the Pile

According to the mechanical model in Fig. 4, the bearing capacity of the discrete material-concrete pile consists of the bearing capacities of the concrete section and the lateral bugling deformation section. In addition, the expression of the overall bearing capacity is shown in Formula (1). Therefore, by comprehensively considering Formulae (1), (2), (20), (21), (23) and (24), the final ultimate bearing capacity of the discrete material-concrete pile can be expressed as follows.

1. If the internal friction angle φ of surrounding soil is zero.

$$Q_p = Q_p' + \tau_u = C_u(\ln I_r + 1)\mathrm{tg}^2\left(45^\circ + \frac{\varphi_p}{2}\right) + \alpha C_u \quad (25)$$

2. When the internal friction angle of surrounding soil is not equal to zero.

$$Q_p = Q_p^{'} + \tau_u = \{(q + C\mathrm{ctg}\varphi)(1 + \sin\varphi)(I_r \sec\varphi)^{\frac{\sin\varphi}{1+\sin\varphi}} - C\mathrm{ctg}\varphi\} \times \mathrm{tg}^2\left(45^\circ + \frac{\varphi_p}{2}\right) + \alpha C_u \quad (26)$$

4 Bearing Capacity of the Surrounding Soil

When the eccentric distance is less than or equals 0.333 times the width of foundation bottom, the characteristic value for the bearing capacity of the foundation is determined according to the shear strength of the soil. Here, the bearing capacity is equivalent to the allowable bearing capacity of the foundation but not the ultimate bearing capacity. The expression is shown in Formula (27).

$$Q_s = M_b\gamma b + M_d\gamma_m d + M_c c_k \quad (27)$$

where Q_s represents the characteristic value (surrounding soil) for the bearing capacity of foundation soil; b is the width of the foundation bottom (when the width exceeds 6 m, it is equivalent to 6 m; for sandy soil, it values 3 m when the width is <3 m); c_k and φ_k are the standard cohesive force and the standard internal friction angle of the soil under the foundation bottom at the depth equal to the width. γ_m represents the weighted average weight of the soil above the foundation bottom (buoyant unit weight is employed when the foundation bottom is below the underground water level); γ is the unit weight of soil below the foundation bottom (buoyant unit weight is employed when the foundation bottom is below the underground water level); M_b, M_d and M_c are bearing capacity coefficients (relating to the internal friction angle of the foundation soil, as shown in Table 1).

When the foundation width is more than 3 m or the burial depth is more than 0.5 m, the bearing capacity characteristic value of the foundation soil calculated using Formula (27) needs to be corrected by

$$Q_s = Q_{sk} + \eta_b\gamma(b - 3) + \eta_b\gamma_m(d - 0.5) \quad (28)$$

where Q_s represents the corrected bearing capacity characteristic value of the foundation soil. Q_{sk} is the bearing capacity characteristic value of the foundation soil; η_b and η_d denote the correction factors for the bearing capacity of the foundation concerning the foundation width and burial depth, respectively.

5 Calculation of Bearing Capacity of the Composite Foundation with New Piles

The bearing capacity of the new composite foundation with discrete material-concrete compound piles is calculated through superposition and combination. In addition, the superposition and combination expression is shown in Formula (29).

$$Q_{cf} = K_1\lambda_1 mQ_p + K_2\lambda_2(1 - m)Q_s \quad (29)$$

where Q_{cf} represents the bearing capacity of the new composite foundation with discrete material-concrete compound piles; Q_p is the bearing capacity of the compound pile; Q_s shows the bearing capacity of the surrounding soil. The other symbols are defined as the above.

Through combination and superposition, the bearing capacity of the new composite foundation with discrete material-concrete compound piles is calculated by the following formulae:

Table 1 Bearing capacity coefficients M_b, M_d and M_c

Standard internal friction angle φ_k of the soil (°)	M_b	M_d	M_c
0	0	1.00	3.14
2	0.03	1.12	3.32
4	0.06	1.25	3.51
6	0.10	1.39	3.71
8	0.14	1.55	3.93
10	0.18	1.73	4.17
12	0.23	1.94	4.42
14	0.29	2.17	4.69
16	0.36	2.43	5.00
18	0.43	2.72	5.31
20	0.51	3.06	5.66
22	0.61	3.44	6.04
24	0.80	3.87	6.45
26	1.10	4.37	6.90
28	1.40	4.93	7.40
30	1.90	5.59	7.95
32	2.60	6.35	8.55
34	3.40	7.21	9.22
36	4.20	8.25	9.97
38	5.00	9.44	10.80
40	5.80	10.84	11.73

1. When the internal friction angle of the surrounding soil is $\varphi = 0$ and the eccentric distance is $\leq$0.033 times the width of the foundation bottom,

$$\begin{aligned} Q_{cf} &= K_1\lambda_1 m Q_p + K_2\lambda_2(1-m)Q_s \\ &= K_1\lambda_1 m\left[C_u(\ln I_r + 1)\mathrm{tg}^2\left(45^\circ + \frac{\varphi_p}{2}\right) + \alpha C_u\right] \\ &\quad + K_2\lambda_2(1-m)(M_b\gamma b + M_d\gamma_m d + M_c c_k) \end{aligned} \tag{30}$$

2. When the internal friction angle of the surrounding soil is $\varphi = 0$ and the foundation width is more than 3 m or the burial depth is more than 0.5 m,

$$\begin{aligned} Q_{cf} &= K_1\lambda_1 m Q_p + K_2\lambda_2(1-m)Q_s \\ &= K_1\lambda_1 m\left[C_u(\ln I_r + 1)\mathrm{tg}^2\left(45^\circ + \frac{\varphi_p}{2}\right) + \alpha C_u\right] \\ &\quad + K_2\lambda_2(1-m)[Q_{sk} + \eta_b\gamma(b-3) \\ &\quad + \eta_b\gamma_m(d-0.5)] \end{aligned} \tag{31}$$

3. In the case that the internal friction angle of the surrounding soil is $\varphi \neq 0$ and the eccentric distance is lower than or equal to 0.033 times the width of the foundation bottom:

$$\begin{aligned} Q_{cf} &= K_1\lambda_1 m Q_p + K_2\lambda_2(1-m)Q_s \\ &= K_1\lambda_1 m\Big\{\Big[(q + C\mathrm{ctg}\varphi)(1+\sin\varphi) \\ &\quad (I_r\sec\varphi)^{\frac{\sin\varphi}{1+\sin\varphi}} - C\mathrm{ctg}\varphi\Big] \\ &\quad \times \mathrm{tg}^2\left(45^\circ + \frac{\varphi_p}{2}\right) + \alpha C_u\Big\} \\ &\quad + K_2\lambda_2(1-m)(M_b\gamma b + M_d\gamma_m d + M_c c_k) \end{aligned} \tag{32}$$

4. When the internal friction angle of the surrounding soil is $\varphi \neq 0$ and the foundation width is more than 3 m or the burial depth is more than 0.5 m,

$$\begin{aligned} Q_{cf} &= K_1\lambda_1 m Q_p + K_2\lambda_2(1-m)Q_s \\ &= K_1\lambda_1 m\Big\{\Big[(q + C\mathrm{ctg}\varphi)(1+\sin\varphi)(I_r\sec\varphi)^{\frac{\sin\varphi}{1+\sin\varphi}} \\ &\quad - C\mathrm{ctg}\varphi] \times \mathrm{tg}^2\left(45^\circ + \frac{\varphi_p}{2}\right) + \alpha C_u\Big\} \\ &\quad + K_2\lambda_2(1-m) \times [Q_{sk} + \eta_b\gamma(b-3) \\ &\quad + \eta_b\gamma_m(d-0.5)] \end{aligned} \tag{33}$$

6 Numerical Simulation of the Composite Foundation with New Piles

For bearing capacity and subsidence calculation of composite foundations, although theoretical analytic calculation can get accurate solutions, the calculated result is not better than that measured in the field bearing capacity and subsidence test. This is because, for the complex and ever-changing engineering practices, field tests are more pertinent. However, because field tests are restricted by various factors, such as long-time consumption and high cost, the method combining theoretical analytic calculation with numerical simulation is more extensively used in geotechnical engineering field.

6.1 Three-Dimensional Mechanical Calculation Model

Different from the mechanical model of a single pile, in the mechanical model of composite foundations,

piles and surrounding soil bear loads together by imposing loads to the bearing plate in the upper foundation. Therefore, the three-dimensional mechanical calculation model built in the study is shown in Fig. 7. In which, the length, width and height of the new composite foundation with discrete material-concrete compound piles are 16, 16 and 15 m, respectively. The concrete section of the compound pile is in a length of 3 m and the concrete grout and gravels are effective connected in a section of 1 m long, while the length of the section with compacted gravels is 7 m.

6.2 Numerical Calculation Model

The numerical model of the new composite foundation with discrete material-concrete compound piles includes 7128 elements and 8396 nodes. The model is a 1/2 symmetric model and the length, width and height of the composite foundation are 16, 8 and 15 m, respectively, while those of the upper bearing plate are 16, 8 and 0.2 m, respectively. In addition, the overall length and diameter of the compound pile are 11 and 0.6 m, respectively. Moreover, the pile is divided into the upper, middle and lower sections, namely concrete section (3 m long), effective connection section of concrete grout and gravels (1 m long), and the 7 m long section with compacted gravels. The boundary constraints of the model are as follows: Z, x and y directions are restricted by the foundation bottom, left and right sides of the foundation, and front and back sides of the foundation, respectively. All the deformation results are output in centimeters.

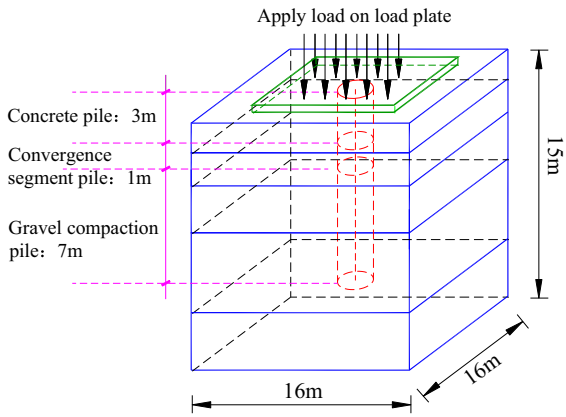

Fig. 7 The three-dimensional mechanical calculation model

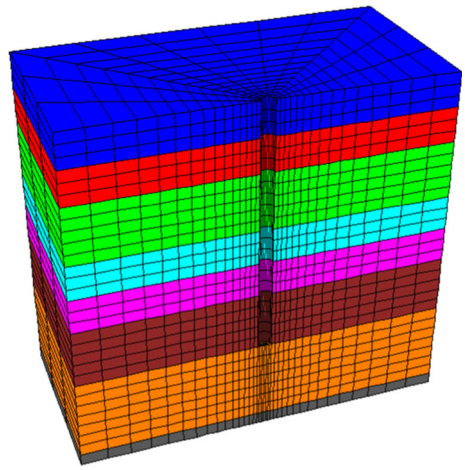

Fig. 8 Pore-forming at the position of the composite foundation pile

Additionally, the establishment and loading of the numerical simulation model are divided into the following eight steps:

Step 1 Establishing the pore-forming model for the position of the composite foundation pile, as shown in Fig. 8.
Step 2 Constructing the model of the first section of the pile with compacted gravels which is suspended above the foundation, as presented in Fig. 9.
Step 3 Placing the above first section of the pile into the composite foundation, as shown in Fig. 10.

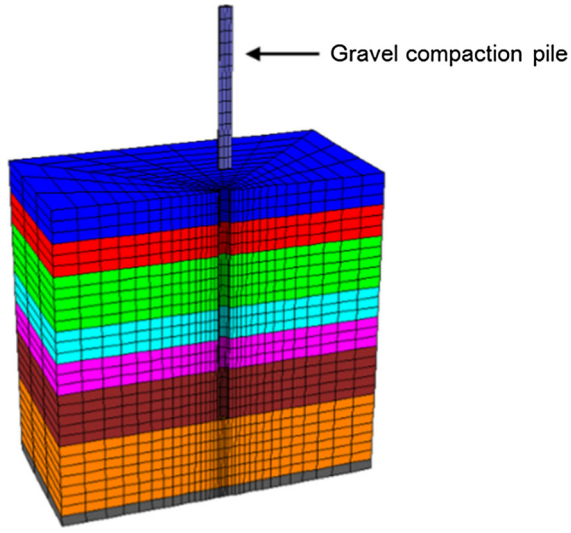

Fig. 9 First section of the pile with compacted gravels suspended above the foundation

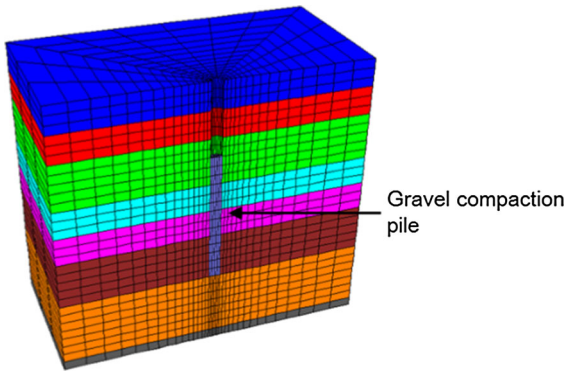

Fig. 10 The first section of the pile with compacted gravels placed into the composite foundation

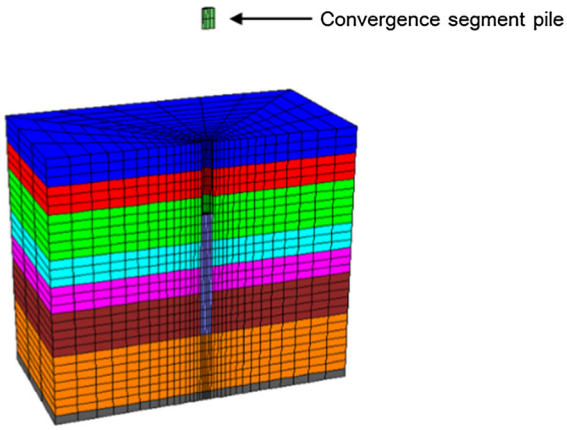

Fig. 11 The second section of the pile with effectively connected concrete grout and gravels suspended above the foundation

Step 4 Establishing and suspending the model of the second section of the pile with effectively connected concrete grout and gravels above the foundation, as illustrated in Fig. 11.

Step 5 Putting the model of the second section of the pile into the composite foundation, as demonstrated in Fig. 12.

Step 6 Building and suspending the model of the third section-concrete section of the pile above the foundation, as shown in Fig. 13.

Step 7 Placing the third section of the pile into the composite foundation, as shown in Fig. 14.

Step 8 Positioning the bearing plate on the top of the composite foundation to form the final loading model, as shown in Fig. 15.

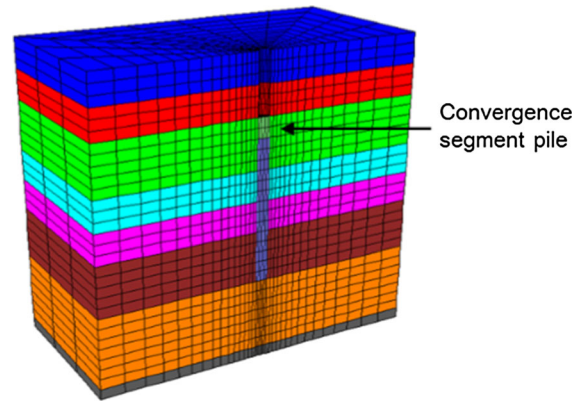

Fig. 12 The second section of the pile put in the composite foundation

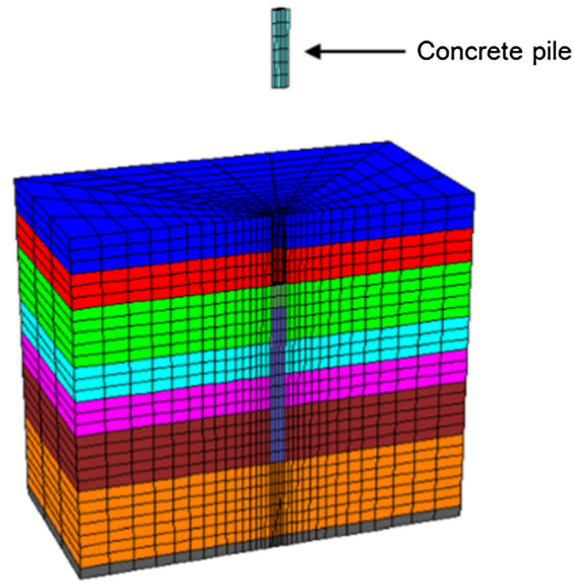

Fig. 13 The third section (concrete section) of the pile suspended above the foundation

6.3 Numerical Calculation Results

The calculation results are listed in Table 2.

6.4 Numerical Calculation Result of the Ultimate Loading Capacity

In order to obtain the ultimate bearing capacity of the new composite foundation, the subsidence of the bearing plate under each grade of loads needs to be extracted. Then according to the subsidence under each

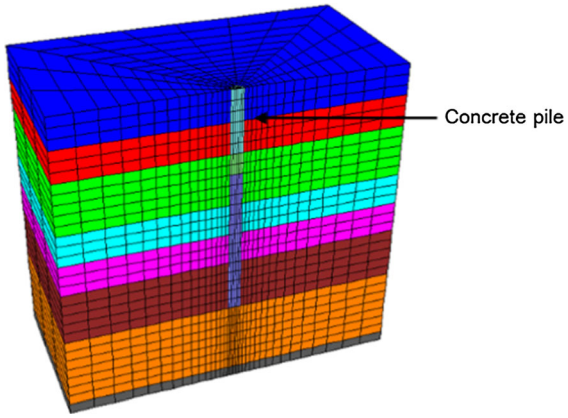

Fig. 14 The third section of the pile placed in the composite foundation

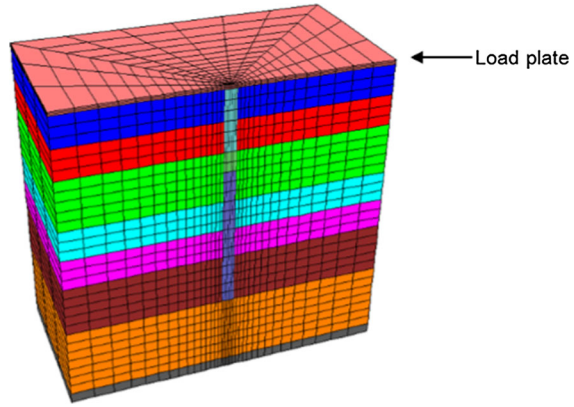

Fig. 15 The final loading model after placing the bearing plate on the top of the composite foundation

grade of loads, the load-subsidence (*P*–*S*) curve is drawn. When *P*–*S* curve sharply declines, it can be inferred that the grade of load is the ultimate load, that is, the ultimate bearing capacity of the new composite foundation. Therefore, according to the numerical calculation result of the new composite foundation under different grades of loads in Table 2, the calculated displacements in the z direction are extracted to draw the *P*–*S* curves, as displayed in Fig. 16.

According to the *P*–*S* curves, it can be inferred that the subsidence of the bearing plate of the composite foundation gradually increases when the loading increases from 50 to 450 kPa. In addition, the subsidence increases smoothly, that is, the subsidence of the bearing plate grows stably, which indicates that the composite foundation is in the normal bearing state. With the load of 450 kPa as the critical point, when the load reaches the value, the composite foundation subsidence suddenly increases from 10.924 to 20.355 cm, almost double of the former. By observing the figure, it is concluded that the section sharply drops in the curve, which suggests that the composite foundation reaches ultimate bearing capacity and is about to experience plastic flow failure. Thus, the ultimate bearing capacity of the new composite foundation is 450 kPa according to the above analysis.

7 Analysis and Discussions

The parameters for numerical simulation calculation in actual engineering are substituted into the analytical formulae for the bearing capacity of the new

Table 2 Numerical calculation results of the new composite foundation under different grades of loads

Load grade (kPa)	Calculated maximum displacement (cm)			Calculated maximum stress (MPa)		
	x direction	*y* direction	*z* direction	*x* direction	*y* direction	*z* direction
50	0.057	0.026	0.840	0.988	0.775	1.700
100	0.083	0.051	1.182	1.142	1.084	1.834
150	0.145	0.084	1.628	1.384	1.2644	2.025
200	0.404	0.316	2.544	1.405	1.330	2.253
250	0.622	0.442	3.575	1.633	1.526	2.557
300	0.756	0.493	4.521	1.859	1.859	2.854
350	0.926	0.5248	6.114	2.110	1.974	3.219
400	1.344	0.839	7.839	2.405	2.280	3.955
450	2.105	1.122	10.924	2.721	2.528	4.664
500	4.734	3.015	20.355	4.102	3.966	8.315

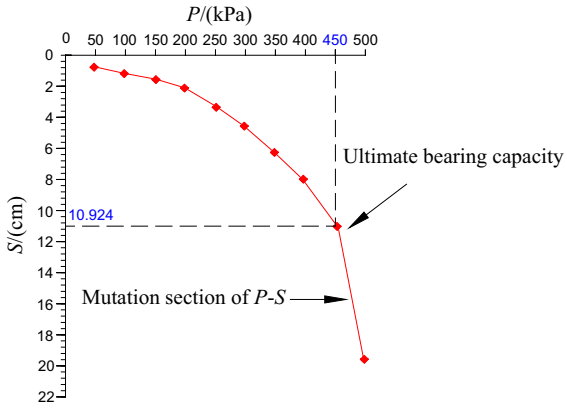

Fig. 16 The loading–subsidence (*P*–*S*) curves of the new composite foundation

composite foundation to obtain the analytical calculation result of the foundation. Then, the analytical calculation result is compared with the ultimate bearing capacity calculated through numerical simulation so as to prove the accuracy of the analytical calculation method. The calculation results are shown in Table 3.

By conducting the analytic calculation and numerical simulation derived from the study, the ultimate bearing capacity of the composite foundation is obtained, respectively. By contrast, it is found that analytic calculation result is close to the numerical simulation result. The analytic calculation result based on the cavity expansion theory is 385 kPa while the numerical simulation result is 450 kPa, which is slightly larger than the former. The former is 14.4% lower than the latter and within the acceptable accuracy range, which proves the accuracy of the analytic calculation method for the bearing capacity of the new composite foundation.

Table 3 Comparison of the results obtained through analytical calculation and numerical simulation

Calculation method	Analytical calculation result (kPa)	Numerical calculation result (kPa)
Ultimate bearing capacity of the new composite foundation	385	450

The analytic calculation result calculated by using the deduced formula in the study is the characteristic value of bearing capacity, while the ultimate bearing capacity can be obtained by multiplying the analytic calculation result by the security coefficient 2. The results in Table 3 are ultimate bearing capacities multiplied by the security coefficient

8 Conclusions

Aiming at the characteristic of the bugling deformation and fracture at the top of gravel piles, a new, optimized composite foundation form was proposed. The composite foundation with compound piles was constructed using discrete materials and concrete piles. Additionally, various parameters of the new composite foundation of discrete material-concrete compound pile were analyzed, including foundation form, construction technologies, bearing mechanism, failure modes and calculation steps for the bearing capacity. The following conclusions were obtained.

1. In the precondition of improving pile strength as well as the vertical and horizontal bearing capacities of the new discrete material-concrete compound pile, the project cost is decreased. In addition, the compound pile has other advantages such as simple construction technology and strong practicability.
2. The bearing mechanism of the discrete material-concrete pile composite foundation is not simple superposition of discrete materials and concrete. However, it is an organic whole of discrete materials, concrete, and surrounding soil constructed by the permeation of the concrete grout to a certain depth of the discrete materials to effectively connect with the latter. Therefore, the compositions are deformed compatibly and bear stress jointly.
3. After analyzing the bearing mechanism and failure modes of the composite foundation with discrete material-concrete compound piles, the bearing capacity of the proposed compound pile is calculated through analytical derivation based on the cavity expansion theory. In addition, the calculation method for the bearing capacity of the surrounding soil is also analyzed. On this basis, the calculation formula for the bearing capacity of the new composite foundation is obtained by using certain superposition principle.
4. The ultimate bearing capacity of the composite foundation is acquired through analytic calculation and numerical simulation separately. It is

found that the analytic calculation result obtained based on the cavity expansion theory is 14.4% lower than that of the numerical simulation result, which is within the acceptable accuracy range. This proves the accuracy of the analytic calculation method for the bearing capacity of the new composite foundation.

Acknowledgements This study is financially supported by the China National Natural Science Foundation (Grants Number 51278187, 51678226); the Natural Science Foundation of Hunan Province (Grant Number 2016JJ4013); the Hunan Science and Technology Project (Grant Number 2014SK3180); the Hunan Provincial Department of Education Science Research Project Key Project (Grant Numbers 15A035, 16A038); the Hunan Provincial Department of Education Science Research Project General Project (Grant Number 16C0304). The authors greatly appreciate the helpful comments and suggestions of the anonymous reviewers.

References

Alamgir M, Miura N, Poorooshasb HB et al (1996) Deformation analysis of soft ground reinforced by columnar inclusions. Comput Geotech 18(4):267–290

Brauns J (1978) Die anfangstraglast von schottersaulen im bindigen untergrund. Die bautechnik 55(8):263–271

Deb K, Mohapatra SR (2013) Analysis of stone column-supported geosynthetic-reinforced embankments. Appl Math Model 37(5):2943–2960

Grujicic M, Pandurangan B, Arakere A et al (2013) Friction stir weld failure mechanisms in aluminum-armor structures under ballistic impact loading conditions. J Mater Eng Perform 22(1):30–40

Hasan KMM, Sarkar G, Alamgir M et al (2012) Study on the quality and stability of compost through a Demo Compost Plant. Waste Manag 32(11):2046–2055

Hughes JMO, Withers NJ (1974) Reinforcing of soft cohesive soils with stone columns. Ground Eng 7(3):42–49

Murugesan S, Rajagopal K (2009) Studies on the behavior of single and group of geosynthetic encased stone columns. J Geotech Geoenviron Eng 136(1):129–139

Poorooshasb HB, Alamgir M, Miura N (1996) Negative skin friction on rigid and deformable piles. Comput Geotech 18(2):109–126

Wang R, Pi J (2011) Comparative analysis of improving soft soil foundation with combining geogrids and gravel piles. Eng J Wuhan Univ 44(1):86–89

Zhao MH, Chen Q, Zhang L et al (2011) Calculation of bearing capacity of geosynthetic-encased stone columns. J Highw Transp Res Dev 28(8):7–12

Zhou ZG, Zhang QS (1997) Analysis of the bearing capacity of geogrid reinforced stone columns. Chin J Geotech Eng 19(1):58–62

Zhuang N, Sun H, Fang J (2016) Stability analysis of aquatic-sand pile composite foundation reinforcing for new shore-connecting structure. Mar Georesour Geotechnol 34(2):106–115